Jet Propulsion Laboratory
California Institute of Technology

4800 Oak Grove Drive
Pasadena, California 91109

(818) 354-4321

JPL

November 5, 1990

To: D. Bagri, W. Brundage, J. Campbell, B. Clark, G. Hunt, P. Napier, K. Sowinski, R. Sramek

From: J. Ulvestad J.U.

Subject: Attached memo on September 28 VLA tests

I enclose a copy of a recently completed memo describing results of a study based on VLA test observations of Jupiter and a calibrator source on September 28. The primary result is that the **A** configuration should be adequate for telemetry reception at Galileo's Io encounter. Autophasing probably can be supported with the **B** configuration, but further work on the correlated noise (from Jupiter) in the telemetry stream is needed to address adequately the feasibility of using the **B** configuration. It may be possible to do some very useful tests in July and October of 1991 by making observations of the Magellan spacecraft in its orbit around Venus.

If you have questions or comments, please feel free to call me at (818) 354-9333, or address me by electronic mail at jsu@grouch (SPAN address GROUCH::JSU).

JET PROPULSION LABORATORY

INTEROFFICE MEMORANDUM

314.5-1492

November 1, 1990

TO: J. W. Layland

FROM: J. S. Ulvestad *JSU*

SUBJECT: September 28 VLA test observations for Galileo Io encounter

Abstract

VLA observations were made of a strong, unresolved radio source that was located only 2 arcminutes from Jupiter on September 28, 1990. This situation was analogous to that on December 7, 1995, when the Galileo spacecraft will encounter Io and Jupiter. The tests showed that, as expected, Jupiter's strong radio emission has a considerable effect on the VLA adjustment of antenna phases for maintaining coherence among the different VLA antennas ("autophasing"). As predicted before the test, Jupiter's effect is rather small for projected baselines longer than ~ 1.1 km in length. A simple emission model has been shown to give a good approximation to the fringe-visibility plots derived from the VLA data. That successful model has been used to generate visibility plots for the encounter with Io and Jupiter and to estimate the VLA's ability to autophase on Galileo during the Io encounter. The most extended configuration of the VLA (the **A** configuration) probably can be used successfully for telemetry reception during the Io encounter.

Further analysis and testing of the effect of correlated noise from Jupiter is necessary before a final decision can be made about the feasibility of using the second largest (**B**) configuration of the VLA for reception of Galileo telemetry. It is suggested that adequate testing could be performed by using the VLA to observe the Magellan spacecraft, which transmits data at X band while it orbits Venus. In particular, the months of July and October 1991 have been identified as times when beneficial tests could be done. At these times, Venus will have the same angular size that Jupiter will have when Galileo arrives, and the VLA will be in its two largest configurations.

I. Introduction

References 1 and 2 described the VLA radio telescope, an aperture synthesis array located west of Socorro, New Mexico. The VLA consists of 27 antennas, 9 on each arm of a Y-shaped configuration. The spacings between adjacent antennas along each arm increase with distance from the center of the array. Four major configurations are employed, **A**, **B**, **C**, and **D**. The respective lengths of each arm in these configurations are 21 km, 6 km, 2 km, and 0.6 km.

The VLA is being investigated for possible use in reception of telemetry from Galileo during its Io encounter in 1995, hours before the closest approach to Jupiter. The VLA would use the spatially unresolved signal from the Galileo spacecraft to adjust the phase calibration of each antenna in order to maintain the coherence among the different antennas of the array. A detailed investigation of this procedure for Voyager 2 at Neptune encounter was reported in reference 3. The "autophasing" procedure relies upon the assumption that the received signal on each interferometer baseline is dominated by a point source, so that phase residuals are dominated by system noise and propagation effects rather than by extended radio emission.

The presence of the strong radio emission of Jupiter places constraints on the ground configuration. The planet Jupiter is an extended radio source with a flux density of ~15 Jy* at X band (8.4 GHz); the exact strength depends on the variable Earth-Jupiter distance. In an observing bandwidth of ~8 MHz, Jupiter's signal is considerably stronger than that expected from Galileo when the spacecraft arrives at the planet. Therefore, the autophasing process can be corrupted by the presence of Jupiter. However, Jupiter is an extended radio source; as baseline lengths are increased, the spatial resolution of Jupiter makes it less important in the autophasing process. A calculation outlined in reference 4 led to the prediction that the effect of Jupiter would be negligible at X band for projected baseline lengths greater than ~ 1.1 km.

On September 28, 1990, Jupiter passed approximately 2 arcminutes from the natural radio source 0839+187 (or 0842+185, if named after its J2000 coordinates). This radio source has an X-band flux density near 1 Jy, similar to the expected Jupiter-encounter value for Galileo in an 8-MHz bandwidth; also, it is an unresolved source as seen by the VLA. Reference 5 described a potential test of autophasing on Galileo, using the VLA to observe this close encounter. That test was carried out on September 28; results and implications of the test are reported in this memo.

* 1 Jy = 10^{-26} W m^{-2} Hz^{-1}

II. Observations

Approximately 70 minutes of VLA time were scheduled on September 28 for X-band observations of Jupiter and 0839+187. The VLA was in a **B/C** hybrid configuration (north arm in the **B** configuration, others in the **C** configuration); projected antenna spacings ranged from about 70 meters to 6.7 km (2,000 to 190,000 wavelengths). During the tests, a point calibrator (0851+202) about 3° from the field of interest was observed in "normal" interferometer mode (with no phase feedback loop) and in autophasing mode, in order to set an approximate flux density scale and to check the system performance. (See §III for further description of these observing methods.) The field including 0839+187 and Jupiter also was observed in both modes in order to provide data for autophasing simulations and to provide real-time autophasing data. Finally, an autophasing observation was made with the VLA split into two subarrays, one containing only antennas with mutual baselines longer than 850 meters, and one containing many antennas near the central hub of the VLA, with a mix of long and short baselines. This last observation was meant to test the real-time performance of the autophasing procedure when only the longer antenna spacings were included.

Figure 1 shows an image of 0839+187 and Jupiter, calibrated using the observations of the nearby calibrator 0851+202. This image has undergone the deconvolution process CLEAN to remove the effects of bad sidelobes in the synthesized VLA beam. The apparently elongated shape of the point source is due to asymmetry in the response function of the VLA, which was caused largely by the north arm of the VLA being much longer than the other two arms during these observations. The *peak* flux density of the point source was a factor of ~ 7 higher than that of Jupiter, because of the resolution of Jupiter with many of the VLA baselines. However, the *total* flux density of Jupiter was much higher than that of the point source.

III. A digression on autophasing

A slight detour is necessary to describe the meaning of "phase" and autophasing in interferometric observations. A two-element interferometer measures the amplitude and relative phase of the cross-correlation of a signal for a pair of antennas. The VLA is a set of 351 simultaneously operating two-element interferometers. The measured phase on each baseline is affected by the geometry of the radio source and the antenna location, propagation effects, instrumental effects, and system noise. Both the propagation effects and many of the instrumental effects are antenna-based in nature; i.e., they are peculiar to a particular antenna and in common to all two-element interferometers including that antenna. The normal "interferometer" mode of the VLA involves no attempt to adjust phases in real time, since those phases carry information about the structure of a radio source which is being mapped by the VLA. Instead, calibration is accomplished by making observations of another (point) radio source, which are used later to solve for the phase calibration peculiar to the individual antennas. The calibration then is applied to the data on the source which is to be mapped.

The purpose of autophasing is to attempt to make all the antennas coherent on a particular source by means of a quasi-real-time phase calibration. This is done for telemetry reception and Very Long Baseline Interferometry, in order to make the VLA mimic one very large antenna of about 130-m diameter. In autophasing, a calibration is made during the observations by assuming that the source being observed is well-represented by a point source. The phases on each baseline are used to construct a least-squares solution that finds the phase calibration peculiar to each antenna, and then remove the antenna-dependent effect from the data in (almost) real time. Both the 351 baseline phases and the 27 individual antenna phase calibrations will be referred to below.

IV. Test results

The results of the observations of 0839+187 were rather confusing. During observations in the autophasing mode, the displayed residual phases for each antenna indicated that each antenna had a small phase residual, as though the autophasing was working well. However, the phases on many individual baselines were quite large and remained relatively constant, sometimes in the vicinity of 60°. (The signal-to-noise ratio of more than 15 to 1 in a 5-second integration on 0839+187 would have given phase residuals on the order of 4° on each baseline if system noise were the limiting factor.) Listing of the phases on all baselines after the experiment indicated high values in many cases. In particular, three antennas moderately close to the center of the array had phases on the order of 90° on baselines with almost every other antenna; the few antennas closer to the center and those farther out had phases on most baselines that were less than 20°.

The real-time phase listing was misleading because the "residuals" displayed actually were just the difference between the antenna phases at the current integration and those predicted based on past integrations. These residuals accurately depict the system performance when the dominant error is dynamic phase fluctuations due to the troposphere or other causes. However, in the situation where the dominant error is an erroneous source model, the antenna phase solutions may not fluctuate greatly from one integration to the next. Thus, the apparent residuals would be small even though the VLA was not maintaining good coherence on the point source.

In the post-processing, attempts to solve for the complex antenna gains (amplitude and phase) from the normal interferometry data gave enormous errors; convergence sometimes did not occur, and no values were reported for the same three antennas that had shown the large phases in the post-experiment phase listings. (Unfortunately, similar failures of convergence are not reported in real time during autophasing.) This may have been due to the confusion caused by the mixture of short and long baselines to these antennas, with the short baselines dominated by Jupiter and the long baselines dominated by the point source 0839+187. Figure 2 shows a portion of the reported errors from the least-squares program that attempts to compute antenna gains; this output is from an individual 5-second integration at 1025 UT. Even for baselines and antennas where the residual phases ostensibly were near zero, it is unclear that the antennas really were in phase with each other. In any case, it was obvious that the autophasing algorithm was strongly affected by the presence of Jupiter.

Off-line gain solutions also were computed for the normal interferometry data using various limitations on the baseline lengths. Elimination of all baselines whose projections were shorter than 30,000 wavelengths gave good results, since the longer baselines detected very little correlated flux from Jupiter. Figure 3 displays the reported errors (with closure limits of 5% in amplitude and 5° in phase) for the gain solutions with this minimum baseline length, using the same 5-second integration as in Figure 2. Although the baseline limitation eliminated some of the 351 baselines from the phase solution, the returned solution gave individual phases for each of the 27 antennas, since even the antennas near the center of the VLA had projected baselines longer than the specified cutoff when combined with the outermost antennas. As long as the solution is not limited by the signal-to-noise ratio on the individual baselines, the solution using a reduced number of baselines should be adequate.

When the VLA was split into two subarrays performing autophasing independently of each other, the subarray containing only baselines longer than 850 meters (most well over a kilometer) performed quite well. No phase residuals larger than 15° were observed either in the real-time autophasing or in the listings generated in the post-processing of the data. Again, this serves to validate the prediction that baselines longer than $\sim$ 1.1 km (30,000 wavelengths) are needed to remove most of the effects of Jupiter.

V. Simulations of test observations and the 1995 encounter

A very useful tool in determining the robustness of autophasing is a plot of the amplitude of the fringe visibility *vs.* baseline length (a "visibility plot"). For observations of a field containing both Jupiter and a point radio source, on baselines long enough that Jupiter is resolved out, the correlated amplitude should be constant with increasing baseline length. Baselines short enough to see a significant correlated amplitude from Jupiter also will have their phases affected by the Jupiter emission. Figure 4 is a visibility plot derived from nine minutes of data taken in the normal interferometer mode. On baselines shorter than about 35,000 wavelengths (1.2 km), the effects of Jupiter are significant. Oscillations in the correlated amplitude are related to alternating constructive and destructive interference between Jupiter and the point source, and die out as baselines become long enough to resolve Jupiter completely. For baselines longer than 30,000–35,000 wavelengths, the flatness of the plot is a result of the absence of significant correlated flux from Jupiter and indicates that autophasing would perform well in this regime.

Figure 5 shows a simulation of a visibility plot using a simple model for the brightness distribution of the point source and Jupiter. The final model included a point source of flux density 0.93 Jy and a uniform disk of total flux density 6.0 Jy. The size of the disk and the source separation were fixed by Jupiter's angular radius and the positions of the point source and the planet, while the baselines sampled were those actually used to acquire the test data illustrated in Figure 4. The flux densities of the sources in the simulation were adjusted to give a good qualitative correspondence between Figures 4 and 5. For each point, 0.054 Jy of noise (computed noise level for the parameters used in the test observations) was added with random phase.

Figure 6 is a comparison of the plots from Figures 4 and 5, and shows the good correspondence between the real data and the simulation. Differences easily can be accounted for by the crude method by which noise was added in the simulation, the fact that different subsets of the real projected baselines were selected for the two plots, and the over-simplification of the uniform disk model for Jupiter. In fact, Jupiter's disk was much stronger than 6 Jy at X band, perhaps 10 Jy or more. However, its large separation from the point source caused it to lie at only about the 65% power point of the VLA antennas, which were pointing at 0839+187. Furthermore, the observed disk was nonuniform in apparent amplitude because the parts located farthest from the point source suffered more dilution by the primary beam of the VLA antennas than did the parts located closest to the point source.

The good correspondence between the real and simulated visibility data indicated that a simple emission model could serve well as a predictor of the visibility function to be expected from the combination of Galileo and Jupiter on encounter day, December 7, 1995. For a total bandwidth of 8 MHz, reference 6 predicts that Jupiter will be about 7.3 times stronger than Galileo in a right-circularly polarized channel of the VLA. When Galileo and Jupiter rise at the VLA, a little less than 3 hours prior to Galileo's closest approach to Io, Jupiter will be located about 51 arcseconds (14 millidegrees) from Galileo. Figure 7 shows the predicted visibility plot for the model of Galileo and Jupiter, assuming use of the **B** configuration of the VLA, in which each of the three VLA arms has a total length of $\sim$ 6 km. More than a third of the baselines will be shorter than 30,000 wavelengths and show a significant effect due to Jupiter. This is partly due to the fact that the spacecraft and Jupiter will be at $-23°$ declination at the encounter. Therefore they rise nearly along the azimuth of the southeast arm of the VLA, giving considerable foreshortening of many baselines. If Jupiter's center and Galileo were located at the same point, this plot would look like a superposition of a constant and a Bessel function $J_1(x)/x$ (where x is the baseline length), the respective Fourier transforms of a delta function and a uniform disk. In fact, the plot is somewhat more complicated because Galileo will not be directly in front of Jupiter, so that Jupiter and Galileo will be beating against each other as Jupiter is being resolved.

Figure 8 shows the visibility plot for the same model as Figure 7, with the exception that the VLA antennas are assumed to be in their most extended arrangement, the **A** configuration. Note that only a few baselines will be short enough to be corrupted significantly by Jupiter.

Figure 9 is a plot similar to Figure 7 for the **B** configuration, except the assumed VLA bandwidth is 3.9 MHz instead of 8 MHz. Figure 10 is the corresponding plot for the A configuration. This situation corresponds to that in which 5 spectral line channels of 781 kHz each, centered on the Galileo carrier, are used for the phase adjustment process. Since Galileo's signal is restricted in frequency, whereas Jupiter is a broadband emitter, this bandwidth gives a higher signal-to-noise on Galileo and a lower signal-to-noise on Jupiter. However, there still is a significant effect caused by Jupiter. The autophasing bandwidth cannot be made much smaller if the first telemetry sidebands are to fall well within the autophasing bandpass.

Figures 11 and 12 plot the visibility functions for the **B** and **A** configurations, respectively, two hours after Galileo and Jupiter rise at the VLA. A 3.9-MHz autophasing bandwidth is assumed. At this time, Galileo will have moved within 19 arcseconds (5 millidegrees) of Jupiter's center, appearing just off the limb of the planet. The spacecraft and Jupiter will be at 25° elevation. Comparison with Figures 9 and 10 shows that the projected baselines will be somewhat longer for the higher spacecraft elevation, and Jupiter's effects on the visibility function will be less pronounced. Thus the limiting case in selection of the appropriate VLA configuration appears to be the situation at the spacecraft rise time.

VI. Discussion

The purpose of the VLA tests and simulations has been to select the appropriate parameters for reception of telemetry from Galileo at Jupiter encounter. There are two issues to be considered. One is the autophasing of the VLA antennas, while the other is the problem of correlated noise from Jupiter in the summed signal from all the antennas. Problems with the autophasing can be reduced by setting a minimum projected length for the baselines used in the autophasing procedure. However, even though this will enable the phase adjustment to converge on antenna solutions that maintain coherence of the signal from Galileo, the close-in antennas still will have small relative phase for some portion of the signal from Jupiter. The contribution of this correlated noise from Jupiter will degrade the signal-to-noise of the telemetry stream. Although the details of correlated noise are beyond the scope of this memo, it is clear that the correlated noise will be minimized when the strength of Galileo relative to Jupiter is maximized. If no baselines show an effect in the visibility plot, there should be little effect from correlated noise. An ideal situation would result from a selection of parameters such that the visibility plots (see Figures 7–12) would be dominated by Galileo and show little effect from Jupiter.

Consider the effect of Jupiter on the visibility function. An arbitrarily selected criterion for minimizing autophasing problems and coherent noise would be to set a dividing line between "good" and "bad" at the point where Jupiter contributes less than $\sim 10\%$ to the total amplitude of the fringe visibility. If Jupiter contributes less than that amount on a given baseline, its contribution to the autophasing error for that baseline will be only $\sim 6°$, and the correlated-noise contribution should be correspondingly small. As is evident from Figure 7, assuming an 8-MHz bandwidth and observations using the **B** configuration, about 150 of the 351 baselines show some effect due to Jupiter. Therefore, this set of parameters is inadequate for telemetry reception from Galileo. Figure 10 shows that for a 3.9-MHz bandwidth and the **A** configuration, no more than 6 baselines will show bad effects due to Jupiter, so this set of parameters could be used for telemetry reception.

The remaining uncertainty is whether both the **A** configuration and the reduced bandwidth are necessary, or if only one change from the parameters of Figure 7 would suffice. Inspection of Figure 9 shows that, with the 3.9-MHz bandwidth and the **B** configuration, only about 20% of the baselines show a contribution of more than 10% due to Jupiter. A rough guess is that the total noise on the telemetry might be a factor of 2–3 higher than that when all noise is completely uncorrelated. For the **A** configuration and the 8-MHz bandwidth, Figure 8 shows a 10% effect on less than 10% of the baselines. These baselines easily can be eliminated in the autophasing solution, but the degradation of telemetry by Jupiter's correlated noise still must be evaluated. The simplest way to do this would be with tests at the VLA that are more complex than the one performed in September. Either a natural radio source containing both point and extended components, or a close passage of Jupiter to another bright, compact radio source might be used to evaluate the noise in the summed signal of all the antennas. However, use of a natural radio source would not give a particularly accurate representation of the distribution of emission from Galileo and Jupiter. The best "near-miss" between Jupiter and a strong point source (P 1352−104) will not occur until late 1993, when the VLA is scheduled to be in the **A** configuration. Even then, the angular separation will be nearly twice as large as the separation in the 1990 test.

An ongoing test opportunity also exists involving the Magellan spacecraft, which transmits an X-band signal to Earth from its orbit around Venus. Appropriate selection of observing parameters probably could be made to mimic the situation when Galileo encounters Jupiter. Parameters that need to be considered include the VLA configuration, the Magellan declination, the Earth-Sun-Venus angle, the Venus flux density, the apparent angular size of Venus, and the spacecraft transmission times compared to its rise times at the VLA. Depending on phase angle, Venus has a brightness temperature of $\sim$ 600 K at 3.6 cm (ref. 7), between 3 and 4 times that of Jupiter. At an Earth-Venus distance of 8.3×10^7 km, Venus has the same angular size ($\sim$ 15 arcseconds) that Jupiter will have when Galileo arrives in 1995; therefore it would have 3–4 times Jupiter's flux density. At this distance, the *total* Earth-received power from Magellan will be approximately 200 times that expected from Galileo on December 7, 1995. However, it may be possible to mimic Galileo's Io encounter by selecting the appropriate bandpass for observations of Magellan, so that only a small fraction of the total power is detected.

In July and October 1991, Venus will have the appropriate angular size of 15 arecseconds and the VLA will be in the **A** (July) and **B** (October) configurations. Although Venus will not be at the right declination to get the same projected baselines that would be appropriate for Galileo's Io encounter, this still would be the best time to do further autophasing tests and investigations of the correlated noise problem. Results of such tests should enable a decision to be made about the feasibility of using the **B** configuration for Galileo's Jupiter encounter.

VII. Summary

A VLA test has been performed which simulated the Galileo-Jupiter encounter that will occur in late 1995. This test showed that the autophasing process is corrupted severely when antennas are spaced closely enough to see a large amount of correlated emission from Jupiter. A simple model of the structure of the radio emission gave good success in reproducing the observed fringe visibility; that model has been used to predict the fringe visibility and the effects of Jupiter at the Galileo encounter. The **A** configuration of the VLA should be adequate to resolve Jupiter enough to minimize both autophasing problems and correlated noise in the telemetry stream. It is doubtful that the **B** configuration is extended enough, but further analysis should be done to investigate the effects of the correlated noise. Observations of the Magellan spacecraft in orbit around Venus could provide important information about the feasibility of usage of the VLA **B** configuration for data return from Galileo at Jupiter. Such tests could be done in July and October of 1991.

I thank Roger Linfield for using his occultation program to identify the close passage between Jupiter and 0839+187 and for searching for similar events with Venus, Jupiter, and Saturn in the 1991–1995 period.

References

1. A. R. Thompson, B. G. Clark, C. M. Wade, and P. J. Napier, "The Very Large Array," *Astrophysical Journal Supplement Series,* vol. 44, p. 151, 1980.

2. P. J. Napier, A. R. Thompson, and R. D. Ekers, "The Very Large Array: Design and Performance of a Modern Synthesis Radio Telescope," *Proceedings of the IEEE,* vol. 71, p. 1295, 1983.

3. J. S. Ulvestad, "Phasing the antennas of the Very Large Array for reception of telemetry from Voyager 2 at Neptune encounter," *TDA Progress Report 42-94,* NASA Jet Propulsion Laboratory, p. 257, April–June 1988.

4. J. Ulvestad, "More on VLA configurations for Galileo's Io encounter," IOM 314.5-1449, June 5, 1990.

5. J. Ulvestad, "Possible test of VLA phasing on a radio source near Jupiter on Sept. 28, 1990," Interoffice Memorandum (unnumbered) to J. Layland, May 24, 1990.

6. J. Ulvestad, "Effects of Jupiter's radio emission on Galileo telemetry reception at non-DSN facilities in the U.S.," IOM 314.5-1442, May 16, 1990.

7. W. M. Kaula, *An Introduction to Planetary Physics: The Terrestrial Planets,* New York: Wiley & Sons, 1968.

cc: Galileo Array Study Team, S. Butman, C. Christensen, R. Dewey, D. Gabuzda, S. Hinedi, R. Linfield, A. Mileant, D. Muhleman, G. Resch, M. Slade, S. Thurman

Figure Captions

1. X-band image of Jupiter and the radio source 0839+187, as taken by the VLA on September 28, 1990.

2. Reported errors from the least-squares solution attempting to compute VLA antenna gains, during a 5-second integration on 0839+187 when it was near Jupiter. All baselines were used in the solution, but only some of the reported errors are shown.

3. Reported errors from the least-squares solution attempting to compute VLA antenna gains, during interferometry observations of 0839+187 when it was near Jupiter. Only baselines with projected lengths longer than 30,000 wavelengths were used. The original data were the same as the data used for Figure 2.

4. Visibility plot for VLA observations of 0839+187 and Jupiter on September 28, 1990.

5. Visibility plot computed from a simple emission model for the VLA test observations on September 28, 1990.

6. Comparison of data (Fig. 4) and simulation (Fig. 5) for the VLA observations on September 28, 1990.

7. Simulated visibility plot for observations of Galileo and Jupiter at their rise time (8° elevation) at the VLA on December 7, 1995. An 8-MHz bandwidth and use of the VLA **B** configuration are assumed.

8. Simulated visibility plot for observations of Galileo and Jupiter at their rise time (8° elevation) at the VLA on December 7, 1995. An 8-MHz bandwidth and use of the VLA **A** configuration are assumed.

9. Simulated visibility plot for observations of Galileo and Jupiter at their rise time (8° elevation) at the VLA on December 7, 1995. A 3.9-MHz bandwidth and use of the VLA **B** configuration are assumed.

10. Simulated visibility plot for observations of Galileo and Jupiter at their rise time (8° elevation) at the VLA on December 7, 1995. A 3.9-MHz bandwidth and use of the VLA **A** configuration are assumed.

11. Simulated visibility plot for observations of Galileo and Jupiter two hours after their rise time at the VLA on December 7, 1995. A 3.9-MHz bandwidth and use of the VLA **B** configuration are assumed.

12. Simulated visibility plot for observations of Galileo and Jupiter two hours after their rise time at the VLA on December 7, 1995. A 3.9-MHz bandwidth and use of the VLA **A** configuration are assumed.

Figure 1. VLA image of 0839+187 and Jupiter
Sept. 28, 1990

PLot file version 3 created 01-OCT-1990 20:49:16
0842+185 IPOL 8436.775 MHZ CLEAN.ICLN.1

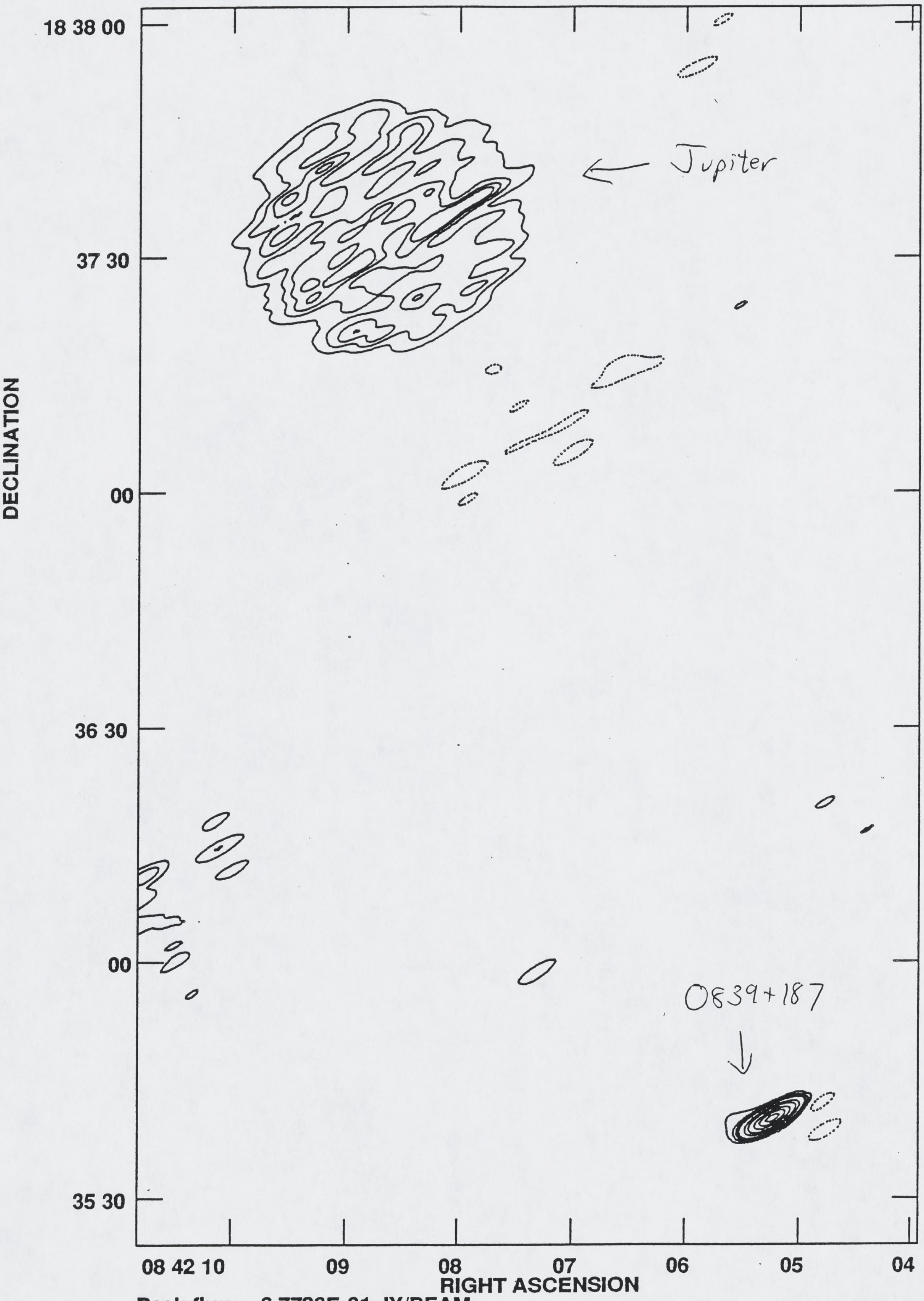

Peak flux = 6.7723E-01 JY/BEAM
Levs = 6.7723E-03 * (-5.00, -2.50, 2.500,
5.000, 7.500, 10.00, 20.00, 30.00, 50.00.

Figure 2. Reported errors from antenna gain solutions on 0839+187, 1025 UT, Sept. 28 1990.

No baseline limitations

```
CALIB                                          begins
CALIB   You are using a non-standard program
CALIB   Selecting and editing the data
CALIB   Dividing data by sourcé flux densities
CALIB   Determining solutions
CALIB   using amp-scalar averaging
CALIB   Writing SN table    1
CALIB   Closure errors at   0/ 10 25  0. 0842+185      IF no.  1  Rpol
CALIB       1-  2  184%   -3d   1-  4  -47%   -9d   1-  5  135%  158d
CALIB       1-  6  163%    1d   1-  7  220%   -9d   1-  8  137%    2d
CALIB       1-  9   84%   22d   1- 10  158%  -31d   1- 11  732%    4d
CALIB       1- 12  327%   16d   1- 13  165%    2d   1- 14  167%   13d
CALIB       1- 15  170%   -6d   1- 16  114%  -17d   1- 17  421% -133d
CALIB       1- 18  -35%  -22d   1- 19  -48%  101d   1- 20  606%   45d
CALIB       1- 21  141%   11d   1- 22  178%   -2d   1- 23  162%   -7d
CALIB       1- 24  -35%  -37d   1- 25  113%  -11d   1- 26  155%   -8d
CALIB       1- 27  190%   -4d   1- 28   -1%   85d   2-  4  -35%    2d
CALIB       2-  5  180%  165d   2-  6  174%    3d   2-  7  237%   -3d
CALIB       2-  8  190%   -3d   2-  9   88%    1d   2- 10  169%   -1d
CALIB       2- 11  129%    1d   2- 12  212%   -5d   2- 13  165%   -4d
CALIB       2- 14  180%   10d   2- 15  167%    2d   2- 16   98%   -6d
CALIB       2- 17  501% -116d   2- 18  -21%  -29d   2- 19  -13%   92d
CALIB       2- 20  234%    3d   2- 21  184%    4d   2- 22  198%    4d
CALIB       2- 23  200%    2d   2- 24  -31%  -32d   2- 25  183%  -14d
CALIB       2- 26  224%   14d   2- 27  206%    4d   2- 28   30%   85d
CALIB       4-  5   24%    7d   4-  6  -32%   -5d   4-  7  -34%   -5d
CALIB       4-  8  -40%   -6d   4-  9  -34%   -7d   4- 11  -53%    3d
CALIB       4- 12  -31%   -8d   4- 13  -36%   -1d   4- 14  -57%    4d
CALIB       4- 15  -33%   -1d   4- 16  -26%   -6d   4- 17  211%   40d
CALIB       4- 19   35%   -9d   4- 20  -33%   -7d   4- 21  -20%   -6d
CALIB       4- 22  -22%   -3d   4- 23  -17%  -19d   4- 24   17%    6d
CALIB       4- 25  -16%    2d   4- 26  -36%   -5d   4- 27  -45%  -11d
CALIB       4- 28    9%  -14d   5-  6  212% -158d   5-  7  333% -162d
CALIB       5-  8  241% -149d   5-  9  124% -155d   5- 11  135% -168d
CALIB       5- 12  260% -153d   5- 13  190% -158d   5- 14   70% -127d
CALIB       5- 15  208% -152d   5- 16  244% -178d   5- 17  323%  107d
CALIB       5- 18  301%   21d   5- 19  268%  -24d   5- 20  194% -144d
CALIB       5- 21  269% -177d   5- 22  303% -153d   5- 23 1711%  138d
CALIB       5- 24  101%   20d   5- 25  412% -164d   5- 26  189% -163d
CALIB       5- 27  211% -162d   5- 28  274%  -46d   6-  7  233%   -4d
CALIB       6-  8  219%    3d   6-  9  105%    2d   6- 10  195%   -9d
CALIB       6- 11  140%    3d   6- 12  210%   -2d   6- 13  205%    0d
CALIB       6- 14  172%    4d   6- 15  207%    7d   6- 16  146%  -10d
CALIB       6- 17  462% -122d   6- 18  -24%  -36d   6- 19   -1%   99d
CALIB       6- 20  184%   -2d   6- 21  164%    7d   6- 22  205%    0d
CALIB       6- 23  208%   -4d   6- 24  -30%  -33d   6- 25  192%  -12d
CALIB       6- 26  184%    4d   6- 27  234%    6d   6- 28   48%   85d
CALIB       7-  8  221%    4d   7-  9   74%    1d   7- 10  229%   -3d
CALIB       7- 11  177%  -11d   7- 12  241%    0d   7- 13  226%   -1d
CALIB       7- 14  380%   -4d   7- 15  198%    2d   7- 16  113%
```

Figure 3. Reported errors from antenna gain solutions on 0839+187, 1025 UT, Sept 28 1990. 30,000 wavelength baseline minimum set

```
145                 01-OCT-1990    23:46:09                  Page    1

       Time           Task         Messages for user  145

990  23:44:54        CALIB      Task CALIB  (release of 15JAN91) begins
990  23:44:54        CALIB      You are using a non-standard program
990  23:44:57        CALIB      Selecting and editing the data
990  23:45:28        CALIB      Dividing data by source flux densities
990  23:45:30        CALIB      Determining solutions
990  23:45:30        CALIB      using amp-scalar averaging
990  23:45:33        CALIB      Writing SN table     1
990  23:45:38        CALIB      Closure errors at  0/ 10 25  0. 0842+185     IF no.  1  Rpol
990  23:45:38        CALIB          1-  7    13%   -5d    1-  8  -11%    3d    1- 21    0%   11d
990  23:45:38        CALIB          2- 16   -16%    6d    2- 18   11%    0d    2- 19  -11%   -3d
990  23:45:38        CALIB          2- 20    17%   -3d    5-  8   13%    7d    7-  9  -15%   -1d
990  23:45:39        CALIB          7- 19   -11%    5d    7- 20  -14%    9d    7- 27  -10%   -2d
990  23:45:39        CALIB          8- 17    -1%   12d    9- 15   11%    1d   12- 17   14%    1d
990  23:45:39        CALIB         13- 27    16%    4d   14- 21  -11%   -3d   15- 19   15%    0d
990  23:45:39        CALIB         15- 22    10%   -4d   15- 28   13%   -3d   16- 26   12%    5d
990  23:45:40        CALIB         21- 26    18%    2d   22- 27  -10%    5d   25- 26   10%   -2d
990  23:45:4[illegible]        CALIB      Closure errors at [illegible]
```

Figure 42. Visibility plot of 0839+187
and Jupiter, September 28 1990

Plot file version 1 created 01-OCT-1990 18:18:06
Amplitude vs UV dist for SUB1.X BAND.1 Source:0842+185
Antennas * - * Stokes I IF# 1
Freq = 8.4368 GHz, Bw = 6.250 MHz
From 0/10:17:05 to 0/10:26:20

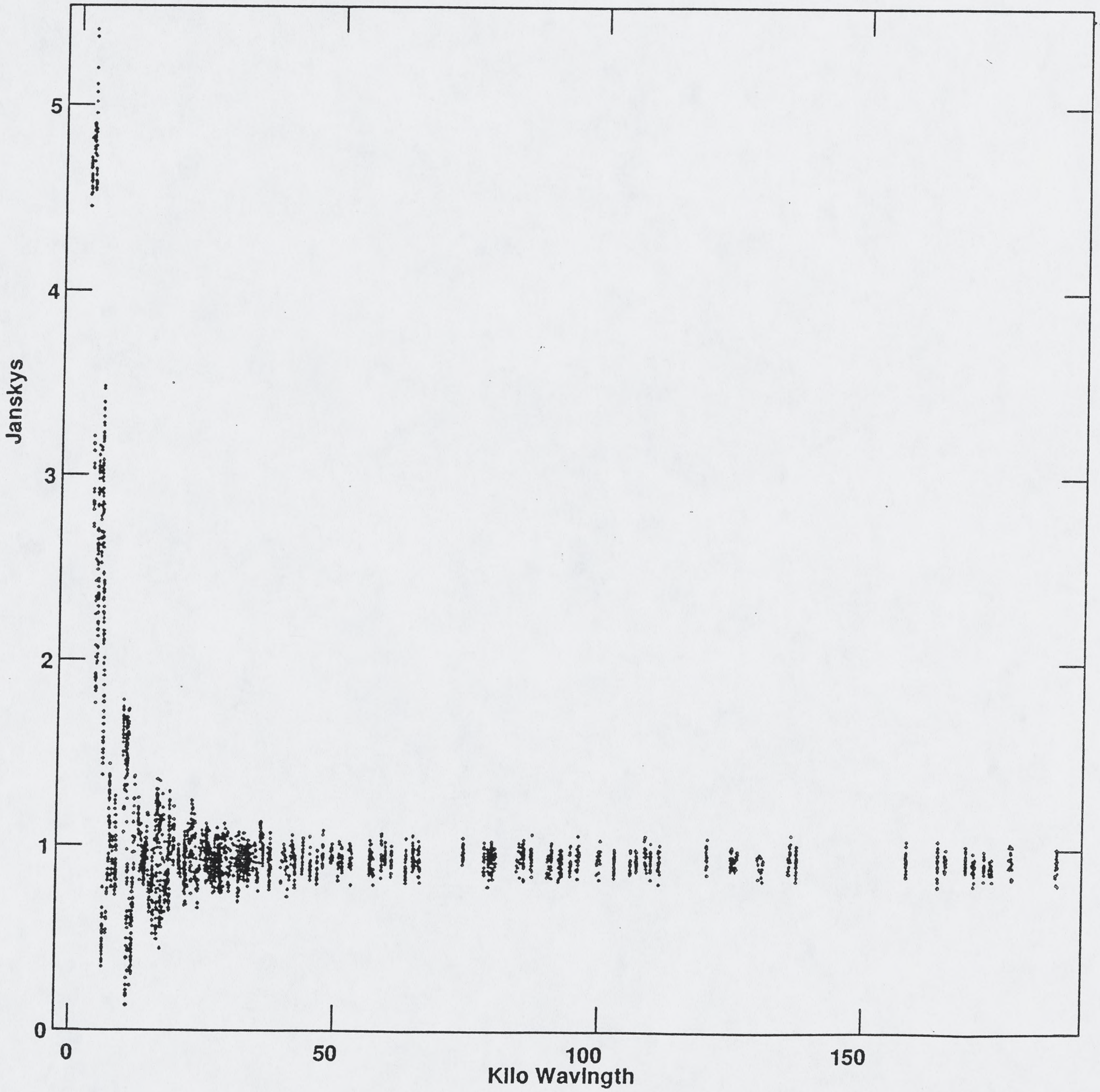

Figure 5. Simulated visibility plot of
0839+187 and Jupiter,
September 28 1990

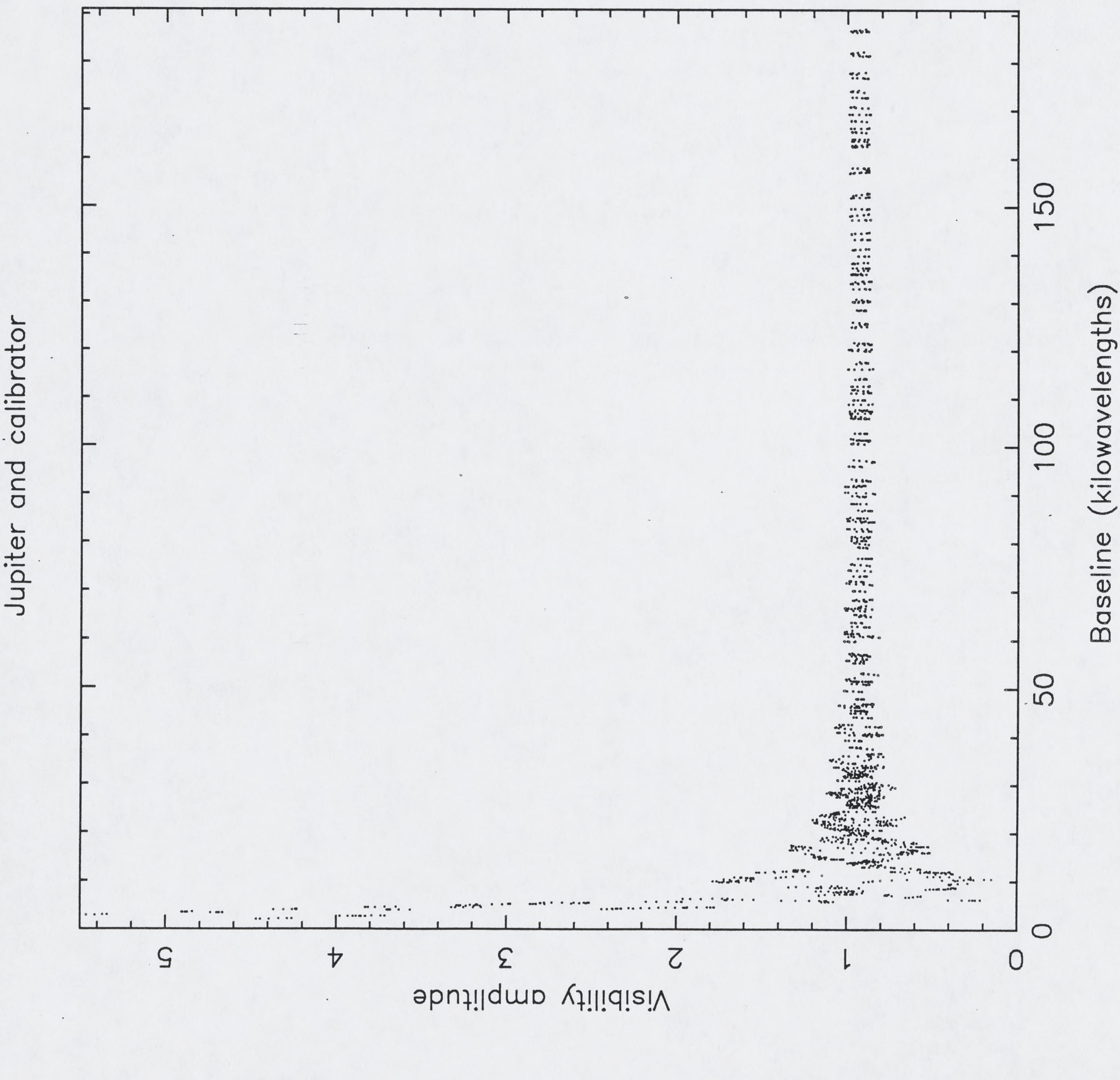

Figure 6. Comparison of real and simulated data on 0839+187 and Jupiter, September 28 1990

Simulated data

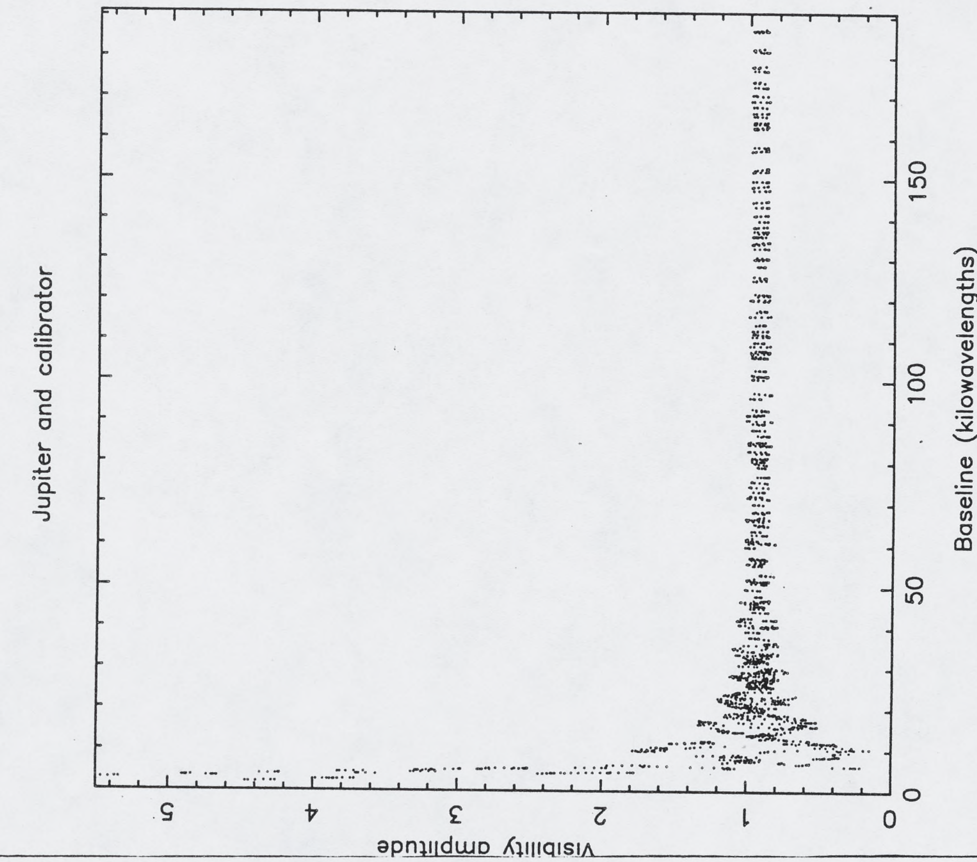

Real data

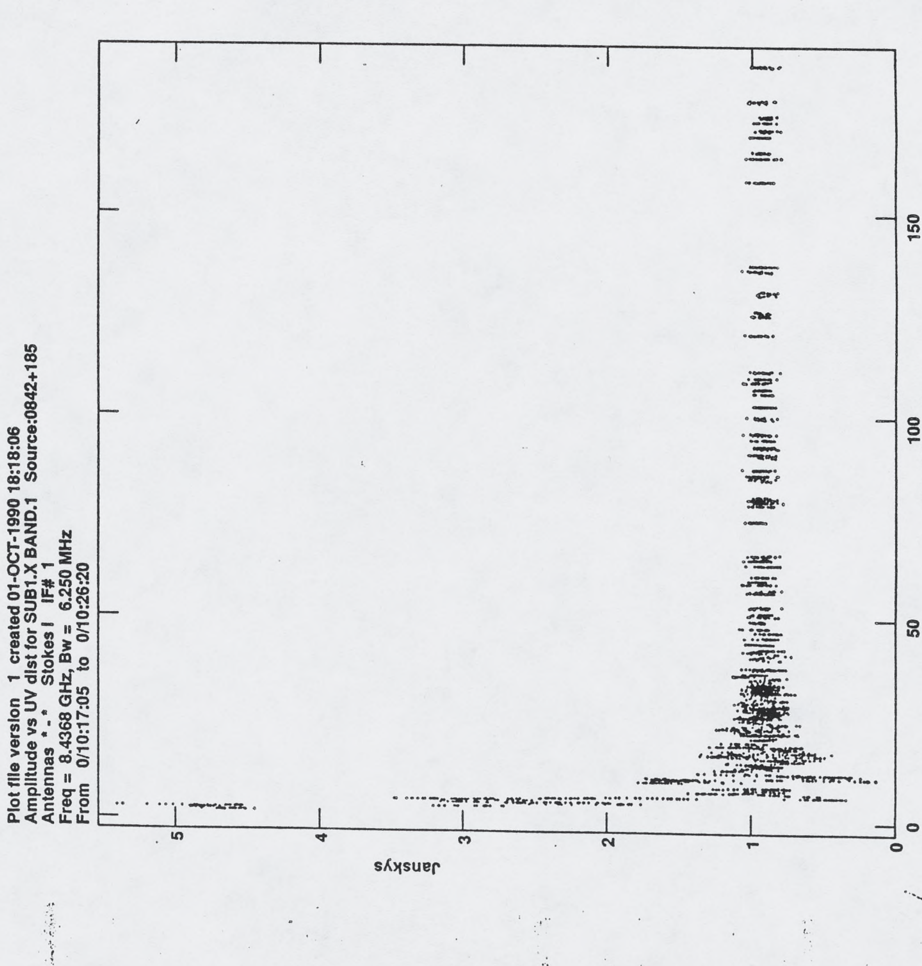

Figure 7. Galileo and Jupiter at VLA
rise time, December 7, 1995
8 MHz bandwidth
B configuration

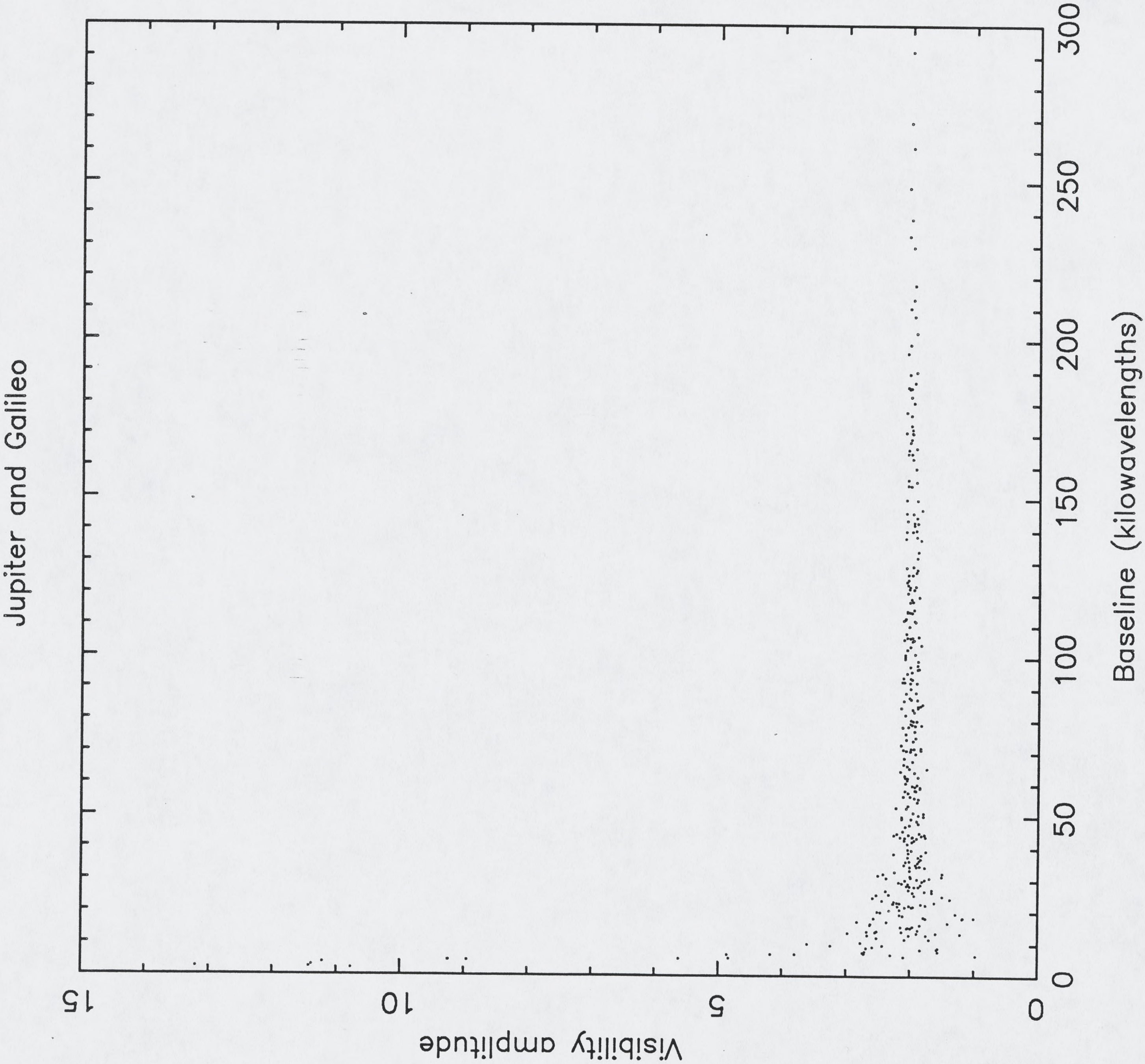

Figure 8. Galileo and Jupiter at VLA rise time, December 7, 1995.
8 MHz bandwidth
A configuration

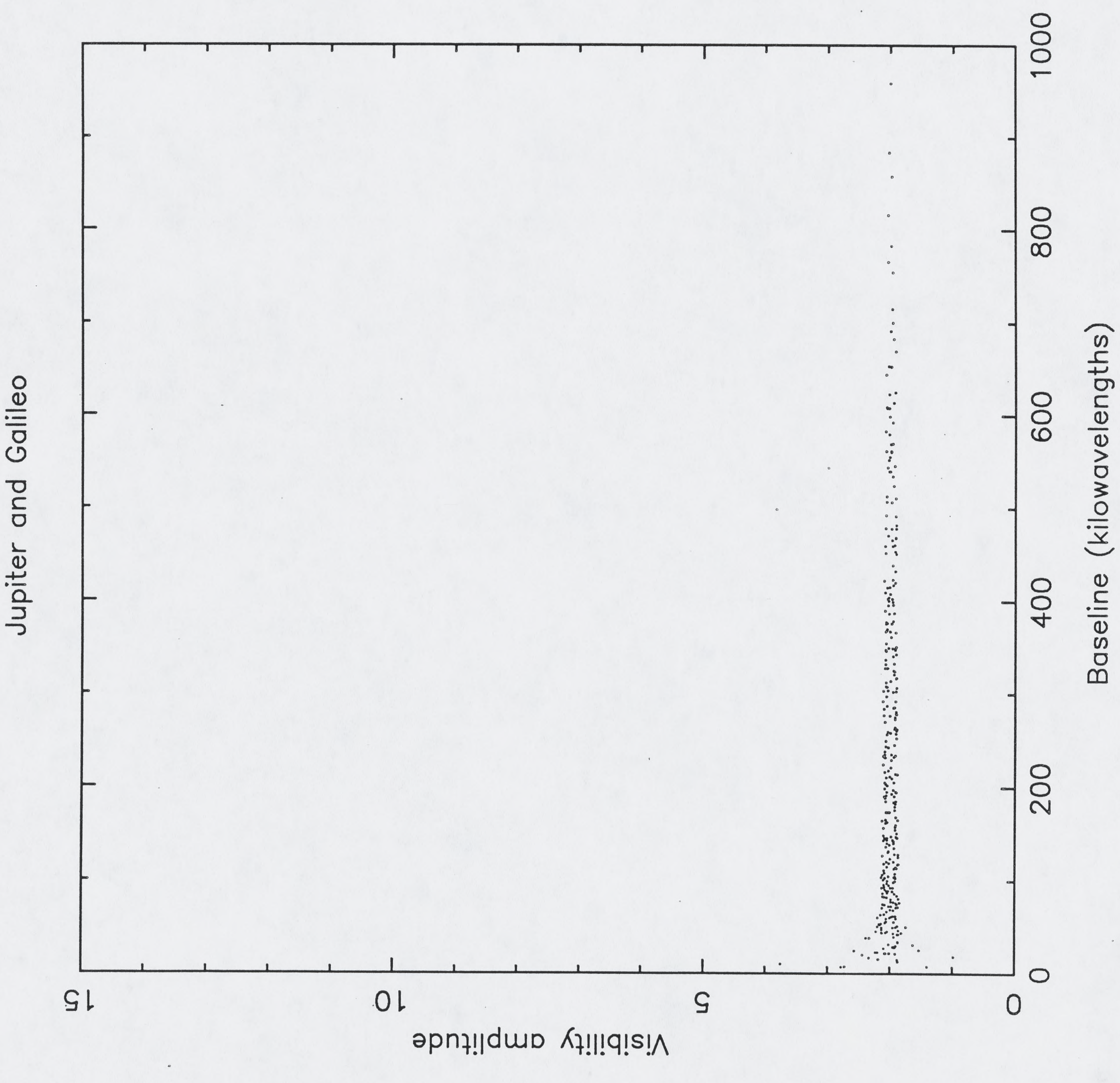

Figure 9. Galileo and Jupiter at VLA
rise time, December 7, 1995
3.9 MHz bandwidth
B configuration

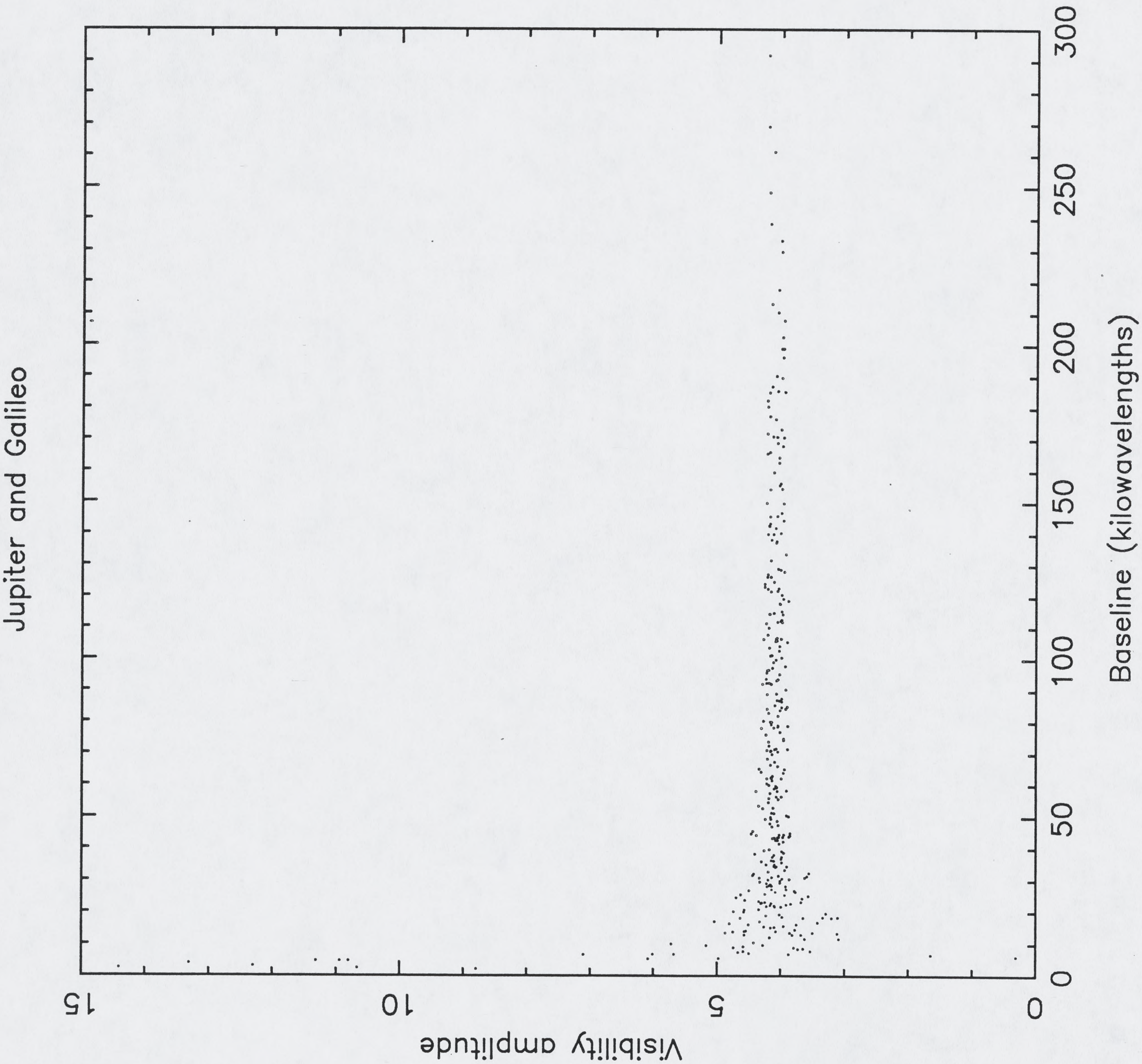

Figure 10. Galileo and Jupiter at VLA rise time, December 7 1995. 3.9-MHz bandwidth A configuration

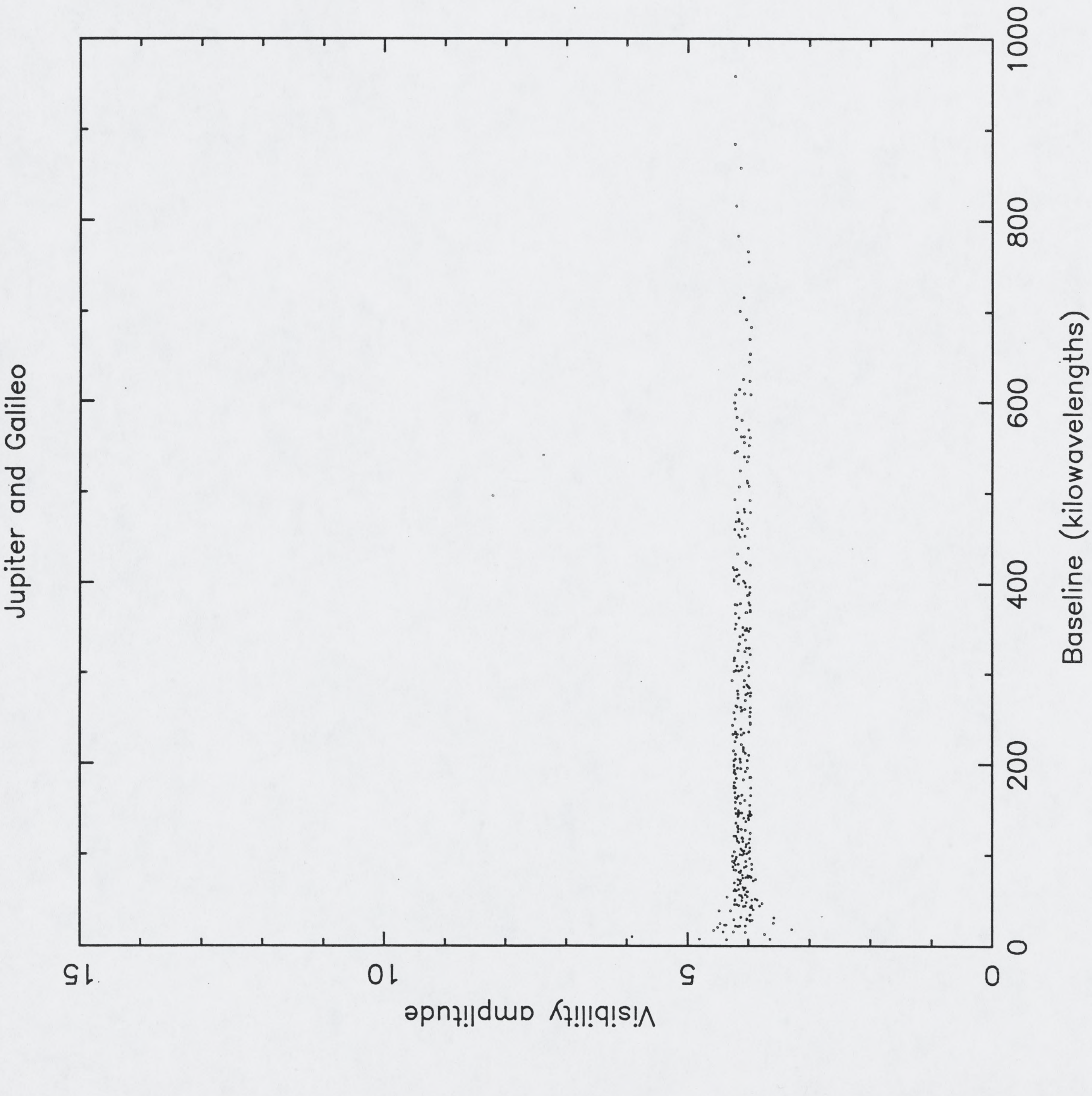

Figure 11. Galileo and Jupiter 2 hours after VLA rise time.
December 7, 1995
3.9- MHz bandwidth
B configuration

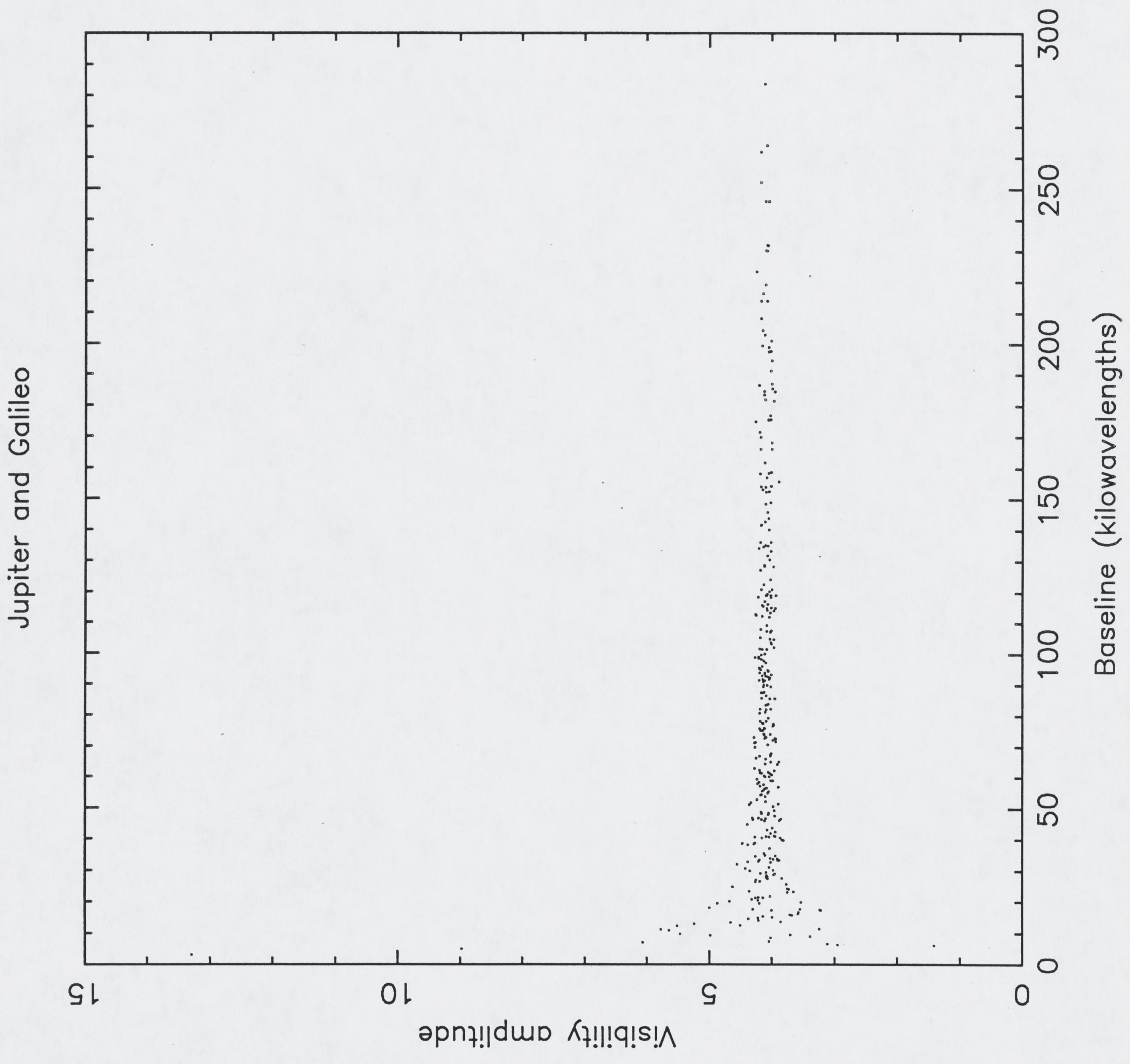

Figure 12. Galileo and Jupiter 2 hours after VLA rise time.
December 7, 1995.
3.9-MHz bandwidth
A configuration